Densely Heterografted Brush Macromolecules with Crystallizable Grafts. Synthesis and Bulk Properties

Dorota Neugebauer,*,† Matthieu Theis, Tadeusz Pakula,‡ and Gerhard Wegner

Max Planck Institut for Polymer Research, P.O. Box 3148, D-55021 Mainz, Germany

Krzysztof Matyjaszewski

Department of Chemistry, Carnegie Mellon University, Pittsburgh, Pennsylvania 15213

Received August 1, 2005; Revised Manuscript Received November 17, 2005

ABSTRACT: Poly(ethylene glycol) methyl ether methacrylate macromonomer (PEOMA, MW = 1100 g/mol, DP_{PEO} = 23) and octadecyl methacrylate or acrylate (ODMA, ODA) were (co)polymerized by atom transfer radical polymerization (ATRP). The one-pot copolymerization via *grafting through* (macromonomer method) yielded densely heterografted copolymers (DP_n = 300−500). The composition of the copolymers strongly depended on the selection of comonomer pairs; i.e., two methacrylates (PEOMA/ODMA) or methacrylate/acrylate (PEOMA/ODA) led to formation of a spontaneous random or gradient copolymer, respectively. The combination of hydrophilic and hydrophobic segments in the same polymer chain caused microphase segregation. Additionally, X-ray results indicated that frustration in packing the crystallizable segments, helical PEOMA and hexagonal ODMA crystals, can direct to an amorphous fraction instead of a semicrystalline ODMA in the graft copolymer. Thermomechanical measurements showed the soft rubbery behavior of the copolymers ($10^4 > G' > 10^3$ Pa, $G' > G''$). The synthesis of homopolymers with a high degree of polymerization is also reported ($DP_{PPEOMA} > 325$, $DP_{PODMA} > 435$, $DP_{PODA} > 150$).

Introduction

Graft copolymers containing a backbone and side chains with a different solid-state nature can phase separate into a wide variety of structures and morphologies. One example is the combination of a crystallizable side chain and an amorphous main chain, which gives copolymers with interesting properties in both solution and bulk. Cooperative organization of the long *n*-alkyl side chains, like in the case of polymers with octadecyl grafts,[1−6] causes crystallization. Poly(octadecyl)-based materials that use cocrystallization with another hydrocarbon to incorporate the material into the same crystalline lattice have found numerous applications as pour-point depressants for lubricating oils or fuels, rheological modifiers, additives in petroleum products, or smart gels.[7] Earlier, conventional radical polymerization and anionic polymerization of octadecyl acrylate and octadecyl methacrylate (PODA, PODMA) yielded ill-defined polymers.[8,9] Recently, successful synthesis of the well-defined octadecyl polymers with various compositions (homopolymers, AB/ABA blocks, statistical and gradient copolymers)[10−14] was performed by atom transfer radical polymerization (ATRP).[15−18]

The controlled ATRP method was also applied to polymerization of biocompatible poly(ethylene oxide) (PEO) macromonomers by *grafting from* or *grafting through*, which led to polymers with a broad variety of compositions. Generally, they can be divided into homografted (all the same PEO side chains) and heterografted (mixture of other grafts with PEO) PEO copolymers. The first group contains polymers with a spectrum of graft density, including loosely grafted polymers (random[19] and gradient[20]) obtained by copolymerization of PEO macromonomer with low molecular weight monomer and homopolymerized poly(PEO macromonomer)s[21] with dense graft distribution, including block copolymers with PEO graft segment.[22] The second group of heterografted PEO materials displays association of crystallizable and hydrophilic PEO side chains with amorphous hydrophobic poly(butyl acrylate) (random composition),[19] polystyrene (alternating copolymers),[23] and PODA (block copolymers)[14] as well as hydrophilic poly(2-hydroxyethyl methacrylate) (brush-*block*-brush)[22] and poly(dimethylsiloxane) (random copolymers).[24] A more complex structure of double-grafted PEO brushes, where each side chain contains PEO grafts, was obtained by grafting the PEO macromonomer from a multifunctional macroinitiator.[21] Both homo- and heterografted PEO brushes can be transformed to a network by chemical or thermal cross-linking and exhibit properties of supersoft rubbers, similar to molecular snakelike brushes with very long backbone and densely grafted P*n*BA side chains.[25]

The structure and crystallization kinetics of linear and triarm star block PEO copolymers composed of two crystallizable blocks of poly(ethylene oxide) or poly(ethylene oxide)−poly(ϵ-caprolactone) and one amorphous polystyrene block have been studied.[26,27] The crystallizable blocks formed multilayer lamellae with a spherulitic superstructure, whereas the amorphous phase was located in the interlamellar PEO regions.

Here, we report results of copolymerization of two crystallizable monomers: hydrophilic poly(ethylene glycol) methyl ether methacrylate, PEOMA (MW = 1100 g/mol, DP_{PEO} = 23), and hydrophobic ODMA or ODA, via *grafting through* using ATRP. The methacrylate comonomers yielded random copolymers P(ODMA-*ran*-PEOMA), whereas copolymers with a spontaneous gradient P(PEOMA-*grad*-ODA) were prepared by copolymerization of the methacrylate/acrylate pair. The combination of two different crystal structures, i.e., helical PEOMA and hexagonal ODMA, is anticipated to influence the morphology of the copolymers in the solid state. Furthermore, each of

† Permanent address: Centre of Polymer Chemistry, Polish Academy of Sciences, 34, Maria Sklodowska-Curie Str., 41−819 Zabrze, Poland.
‡ Deceased.
* Corresponding author. E-mail: dorotaneu@poczta.onet.pl.

10.1021/ma051702h CCC: $33.50
Published on Web 12/22/2005

the monomers was homopolymerized to obtain polymers with uniform graft structure: PODMA, PODA, and PPEOMA. The modified conditions developed the length of polymer backbone with larger DP_n compared to polymers described earlier in the literature. The properties of homo- and heterografted PEO−OD (co)polymers were investigated by differential scanning calorimetry (DSC), X-ray scattering methods (WAXS, SAXS), and dynamic mechanical measurements (DMA). The copolymers containing PEO segments are supersoft elastomeric materials with very low shear modulus $G' = 10^3-10^4$ Pa, where $G' > G''$.

Experimental Section

Materials. Poly(ethylene glycol) methyl ether methacrylate, $H_2C{=}C(CH_3)COO-(CH_2CH_2O)_{23}CH_3$ (PEOMA, MW_{av} = 1100 g/mol), octadecyl acrylate, and methacrylate (ODA, ODMA) were obtained from Aldrich. The solid monomers were dissolved in THF and passed through an alumina column to remove the antioxidant inhibitor (MEHQ and BHT), and then the solvent was evaporated and the monomer was dried under vacuum to a constant mass. Copper(I) bromide (CuBr, Aldrich, 98%) and copper(I) chloride (CuCl, Acros, 95%) were purified by stirring with glacial acetic acid (Fisher Scientific), followed by filtration and washing the solid three times with ethanol and twice with diethyl ether. The solid was dried under vacuum (1×10^{-2} mbar) for 2 days. Copper(II) bromide ($CuBr_2$, Acros, 99+%) was used as received.

4,4′-Di(5-nonyl)-2,2′-bipyridyne (dNbpy)[28] and tris(2-dimethylaminoethyl)amine (Me_6TREN)[29] were prepared as previously described. Ethyl 2-bromoisobutyrate (EtBriBu, Aldrich, 99%), all solvents, and internal standards were used without purification.

Synthesis. *Synthesis of (Co)polymers.* The (co)monomer(s) dissolved in solvent and added ligand (dNbpy or Me_6TREN) were degassed by three freeze−pump−thaw cycles. After that, CuX (X = Br, Cl) was introduced, and the mixture was stirred for 10 min at room temperature. Next, the mixture in the Schlenk flask was placed in a thermostated oil bath at 90 °C, and EtBr*i*Bu was added after 1 min to start the polymerization. During the polymerization, samples were taken periodically for GPC and NMR analyses. The reaction was stopped by exposing the solution to air, and then the mixture, diluted with THF, was filtered through an activated (neutral) alumina column to remove the copper catalyst. The remaining unreacted monomer was removed by ultrafiltration in THF solution using a membrane (Millipore, regenerated cellulose, YM10, NMWL: 10 000). The graft copolymers were dried under vacuum at room temperature to a constant mass.

Homopolymers were precipitated, after filtration, in hexane from ethanol (PPEOMA) or in methanol from THF (PODMA and PODA).

Characterization. *Gel permeation chromatography (GPC)* measurements were conducted in THF at 30 °C using a Waters 515 liquid chromatograph pump (1 mL/min) and four Polymer Standards Service columns (guard, 10^5 Å, 10^4 Å, 10^3 Å) in series with three detection systems: a differential refractometer (Waters model 410), a differential viscometer (Viscotek model H502), and multiangle laser light-scattering (MALLS) detector (DAWN model F) in the case of copolymers. The determination of apparent molecular weights for the homopolymers was based on linear poly(methyl methacrylate) (PMMA) standards. The refractive index increment d*n*/d*c* was determined with an Otsuka Photal RM-102 differential refractometer.

^{1}H nuclear magnetic resonance (NMR) spectroscopy was performed on a Bruker 300 MHz spectrometer in chloroform-*d* at room temperature.

Differential scanning calorimetry (DSC) was performed with a Mettler 30 calorimeter. Heating and cooling runs were performed at a rate of 1 °C/min in the temperature range −60 to 75 °C.

Wide-angle X-ray diffraction (WAXS) and small-angle X-ray scattering (SAXS) were used to characterize the structure of the bulk materials. In both cases, Cu Kα radiation (λ = 0.154 nm) was used with pinhole collimation and 2D position-sensitive detector (Siemens). The recorded scattered intensity distributions were integrated over the azimuthal angle and are presented as functions of the scattering vector ($s = 2 \sin\theta/\lambda$, where θ is the scattering angle). Measurements were performed at various temperatures. Furthermore, 2D-WAXS experiments allowed to observe scattering patterns, which give information about distance and orientation correlations. Polymer samples were prepared by the extrusion method close to the melting point in order to obtain oriented fibers.

Polarized Optical Microscopy (POM). A Zeiss (D-7082) microscope equipped with a temperature-controlled stage (Linkam TMS91/THM600) and a color digital camera was used for the measurements.

Dynamic mechanical analysis (DMA) was performed using a mechanical spectrometer (RMS 800, Rheometic Scientific). Temperature dependencies of the complex shear modulus were measured at a constant deformation frequency of 10 rad/s. Cooling or heating rates were 2 °C/min.

Scheme 1. Schematic Depiction of the (Co)polymers with Various Compositions Prepared by ATRP

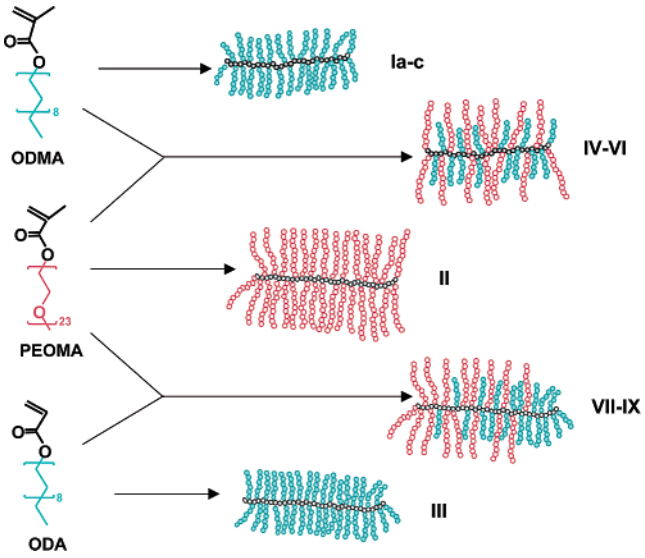

Table 1. Polymerization of ODMA, PEOMA, and ODA

		NMR		GPC	
no.[a]		conv (%)	DP_n	$M_{n,ap} \times 10^{-3}$ (g/mol)	M_w/M_n
Ia	PODMA	41.0	165	41.2	1.25
Ib		45.0	225	74.4	1.15
Ic		66.9	435	148.1	1.31
II	PPEOMA	71.8	323	123.1	1.06
III	PODA	29.5	147	41.3	1.50

[a] (**Ia**) $[ODMA]_0:[EtBriBu]_0:[CuBr]_0:[CuBr_2]_0:[dNbpy]_0 = 400:1:1:0.05:2$; 90 °C; mon/*o*-xylene = 1/1 w/v; (**Ib**) $[ODMA]_0:[EtBriBu]_0:[CuBr]_0:[CuBr_2]_0:[dNbpy]_0 = 500:1:1:0.01:2$; 90 °C; mon/*o*-xylene = 1/1 w/v; (**Ic**) $[ODMA]_0:[EtBriBu]_0:[CuBr]_0:[CuBr_2]_0:[dNbpy]_0 = 650:1:1:0.01:2$; 90 °C; mon/*o*-xylene = 1/0.5 w/v; (**II**) $[PEOMA]_0:[EtBriBu]_0:[CuCl]_0:[Me_6TREN]_0 = 450:1:2:2$; 90 °C; mon/anisole = 1/1 w/v; (**III**) $[ODA]_0:[EtBriBu]_0:[CuCl]_0:[Me_6TREN]_0 = 500:1:2:2$; 90 °C; mon/*o*-xylene = 1/1 w/v.

Results and Discussion

(Co)polymers of ODMA and PEOMA. ODMA was used previously for the preparation of polymers with relatively short blocks, $DP_n < 100$, using EtBr*i*Bu/CuBr/$CuBr_2$/dNbpy in *o*-xylene at 90 °C.[12] The results for homopolymers **Ia**−**c** (Scheme 1) presented in Table 1 were obtained for reactions performed under similar conditions. The initial ratio of monomer/initiator was adjusted to yield longer chains; however, this decreased the reaction rate; i.e., merely 40% monomer conversion was observed after a few days for PODMA **Ia**. The amount

Table 2. Copolymerization of PEOMA (A) and ODMA (B)

		NMR			GPC-MALLS				
			DP_n					DP_n	
no.[a]	PEOMA/ODMA wt % (mol %)	conv (%)	A	B	$M_n \times 10^{-3}$ (g/mol)	M_w/M_n	d*n*/d*c*[b] (mL/g)	A	B
IV	25/75 (10/90)	87.0	41	394	337	1.41	0.077	76	747
Va	53/47 (25/75)	56.6	76	207					
Vb		97.1	120	365	283	1.39	0.074	129	392
VI	75/25 (50/50)	80.5	209	193	287	1.08	0.07	212	196

[a] **(IV, Vb, VI)** $[PEOMA + ODMA]_0:[EtBr\mathit{i}Bu]_0:[CuCl]_0:[Me_6TREN]_0 = 500:1:2:2$; 90 °C; mon/solv = 1/1 w/v; solv = anisole/*o*-xylene (1/1); (**Va**) $[CuBr]_0:[CuBr_2]_0:[dNbpy]_0 = 1:0.01:2$. [b] THF, d*n*/d*c* (PPEOMA) = 0.068 mL/g and d*n*/d*c* (PODMA) = 0.08 mL/g.

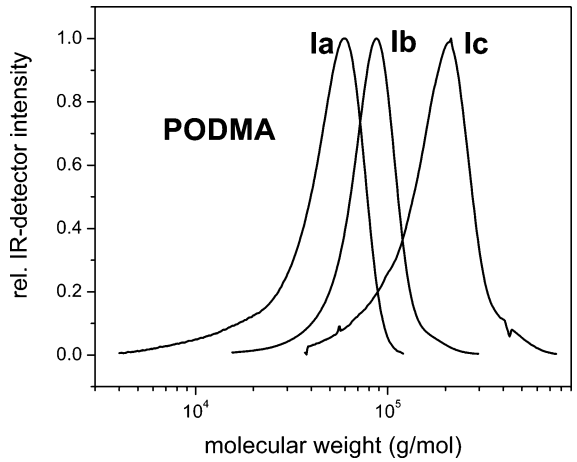

Figure 1. GPC traces of PODMA. Polymerization conditions: $[ODMA]_0:[EtBr\mathit{i}Bu]_0:[CuBr]_0:[dNbpy]_0:[CuBr_2]_0 = 400$(**Ia**)/500(**Ib**)/650(**Ic**):1:1:0.05(**Ia**)/0.01(**Ib**, **Ic**); ODMA/*o*-xylene = 1/1 (**Ia**, **Ib**) or 1/0.5(**Ic**) w/v; $T = 90$ °C.

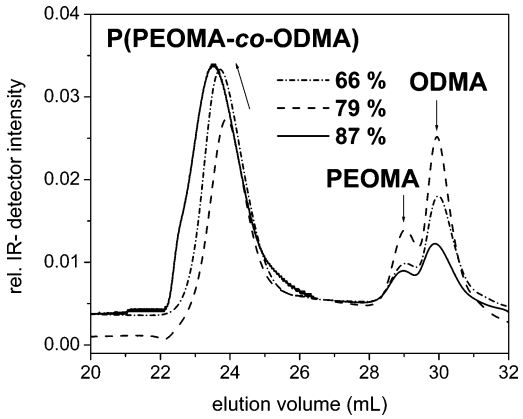

Figure 2. GPC traces for copolymerization of PEOMA and ODMA (**IV**). Conditions: $[PEOMA + ODMA]_0:[EtBriBu]_0:[CuCl]_0:[Me_6TREN]_0 = 50 + 450:1:2:2$; (PEOMA + ODMA)/(anisole + *o*-xylene) = 1/(0.25 + 0.75) w/v; $T = 90$ °C.

of the deactivator, $CuBr_2$, was reduced to 1% in the next set of experiments to shorten reaction time, and additonally, a less dilute system (twice less solvent) directed to production of polymers **Ib** and **Ic** with higher DP_n, above 400, and monomer conversion up to 67%. Figure 1 illustrates that all polymers with various DP_n displayed monomodal GPC traces. In the case of PODMA, **Ia,** with the lowest molecular weight (MW), some tailing is visible, which increased polydispersity index ($M_w/M_n = 1.25$). For PODMA **Ib** and **Ic** with higher MW the values of polydispersity were in the range 1.15−1.3.

The polymerization of the second crystallizable monomer PEOMA (MW = 1100 g/mol, $DP_{n,PEO} = 23$) with CuBr/dNbpy in anisole led to low monomer conversion of 25% ($DP_n = 60$), whereas use of the CuBr/EHA_6TREN system (EHA_6TREN = tris(2-ethylhexyl acrylate aminoethyl)amine) enhanced the polymerization, resulting in PPEOMA with $DP_n = 204$ and $M_w/M_n = 1.47$.[21] In the present work, EHA_6TREN was replaced by another ligand from the TREN family, i.e., Me_6TREN,[30] which yielded polymacromonomer **II** with significantly narrower molecular weight distribution (MWD), $M_w/M_n < 1.1$ for $DP_n > 300$ at above 70% monomer conversion (Scheme 1, Table 1).

The more active system, with Me_6TREN as ligand, was also used for polymerization of ODA which has lower reactivity than methacrylate. The polymerization was stopped at low conversion, 30% ($DP_n = 150$), and it resulted in polymer **III** (Scheme 1, Table 1) which had the broadest MWD among all the homopolymers prepared in this study ($M_w/M_n = 1.5$). This could be due to lower solubility of Cu/Me_6TREN complexes in nonpolar media.

The copolymerization of two methacrylates, ODMA and PEOMA, was performed with the system that was efficient for homopolymerization of ODMA, EtBriBu/CuCl/dNbpy. Under these conditions 57% of the comonomers were converted into polymer P(ODMA-*co*-PEOMA), **Va**, within 47 h. Use of a more active catalyst, CuCl/Me_6TREN in a mixture of anisole/*o*-xylene at 90 °C, improved the yield to a conversion of 80−95% for copolymers **IV**, **Vb**, and **VI** within several hours (Table 2). The progress of reaction, followed by GPC chromatograms, is presented in Figure 2 which are representative for copolymerization with excess ODMA (**IV**, 75 wt % = 90 mol %). The intensity of the signals assigned to the comonomers decreased as the reaction progressed, whereas the copolymer peak increased in intensity as the reaction shifted to higher MW. The level of control was better with higher concentrations of PEOMA in the feed. Copolymers with less PEOMA resulted in higher polydispersity and higher molecular weight than predicted, which could be due to lower initiation efficiency and more significant termination.

Conversion during polymerization was determined using ^1H NMR (Figure 3). Unfortunately, some signals from oxymethylene protons $-O-CH_2-CH_2-$ belonging to ODMA monomer ($\delta = 4.06$ ppm; *c*′) and to PEOMA units in the formed copolymer ($\delta = 4.02$ ppm; *i*) overlapped, making it impossible to distinguish them as separate peaks. A similar situation was observed for oxymethylene protons $-O-CH_2-CH_2-$ present in PEOMA monomer ($\delta = 3.72$ ppm; *d*) and methylene protons $-O-CH_2-CH_2-CH_2-$ in ODMA units of the formed copolymer ($\delta = 3.80$ ppm; *i*′). Additionally, methyl ($\delta = 1.25$ ppm; *h* and *h*′) and methylene (δ (ppm) = 1.64 and 1.83; *g*, 1.71 and 1.90; *g*′) protons in the copolymer backbone overlapped with protons in monomers (δ (ppm) = 1.00−1.40; *e*, and 1.77; *b*, 1.87; *b*′, respectively). However, the comparison of the peak area of the signal assigned to the methoxy protons $-O-CH_3$ ($\delta = 3.35$ ppm; *f*) of PEOMA in the monomer and copolymer with the oxymethylene protons $-O-CH_2-CH_2-$ ($\delta = 4.27$ ppm; *c*) or with the vinyl protons $CH_2=C-$ ($\delta = 5.54$ and 6.10

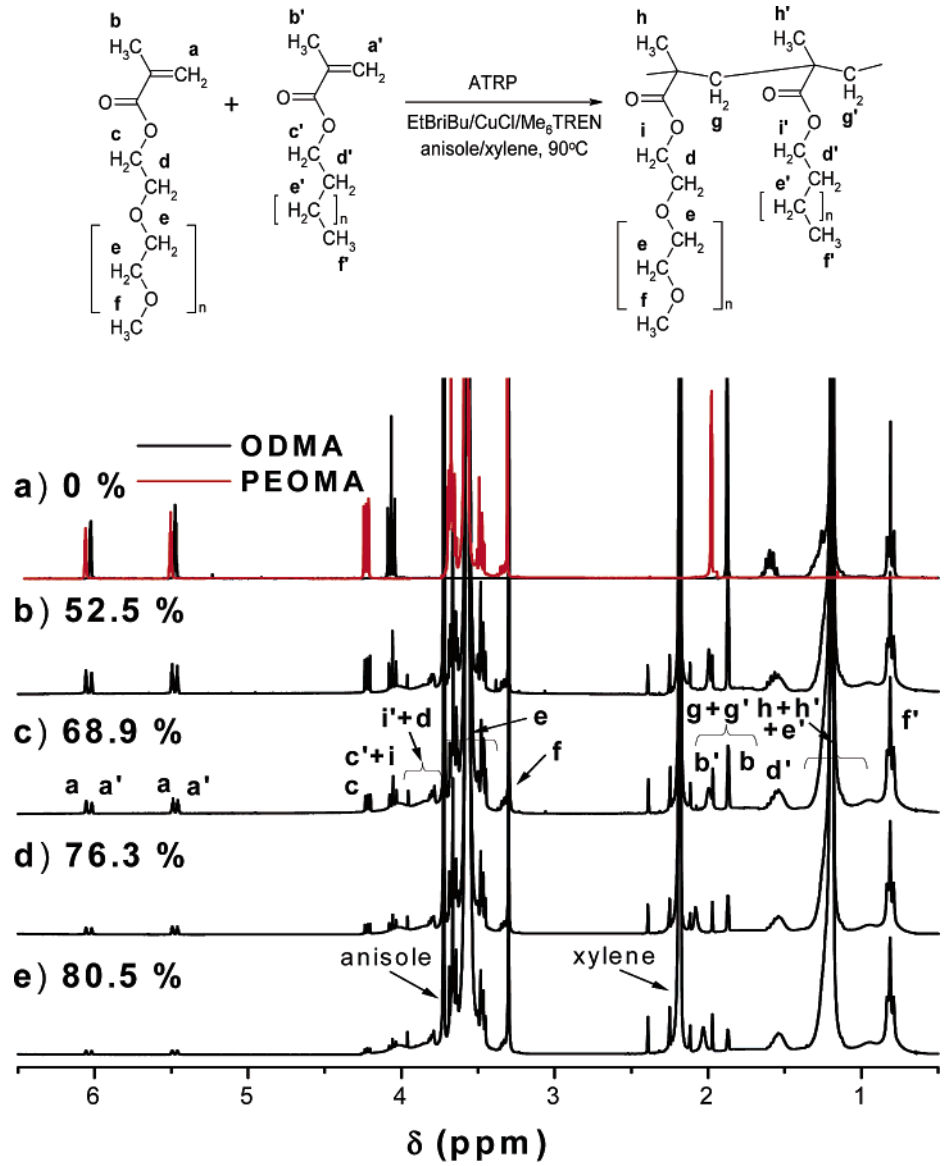

Figure 3. ^{1}H NMR spectra for copolymerization of PEOMA and ODMA (**VI**). Conditions: [PEOMA + ODMA]$_0$:[EtBriBu]$_0$:[CuCl]$_0$:[Me$_6$-TREN]$_0$ = 250 + 250:1:2:2; (PEOMA + ODMA)/(anisole + *o*-xylene) = 1/(0.5 + 0.5) w/v; T = 90 °C.

ppm; *a*) in the monomer allowed calculation of PEOMA conversion. For ODMA, the signal of methylene protons −O−CH$_2$−C*H*$_2$− (δ = 1.59 ppm; *d*′) in monomer and copolymer was compared with monomer signals ascribed to vinyl protons CH$_2$=C− (δ = 5.47 and 6.03 ppm; *a*′).

The semilogarithmic plot of monomer consumption vs time in Figure 4 shows that polymerization of PEOMA and ODMA proceeded at similar rates, reaching high conversions, p_{PEOMA} = 0.83 and p_{ODMA} = 0.82 after 3 h for polymer **IV**. This indicates a random composition of the copolymers P(ODMA-*ran*-PEOMA) (**IV**−**VI**, Scheme 1).

Copolymers Containing ODA and PEOMA. Using similar conditions (EtBr*i*Bu/CuCl/Me$_6$TREN, anisole/*o*-xylene, 90 °C), copolymerization of the same PEO macromonomer (MW = 1100 g/mol) with ODA resulted in copolymers with two kinds of grafts, hydrophilic PEO and hydrophobic C18 aliphatic chains. However, the selection of the methacrylate/acrylate comonomer pair caused the formation of copolymers with a different composition than described above. Conversion of the comonomers was also determined by ^{1}H MNR in the same way as for the random copolymers. The kinetics of the polymer formation, exemplified in Figure 5, indicated that PEOMA was

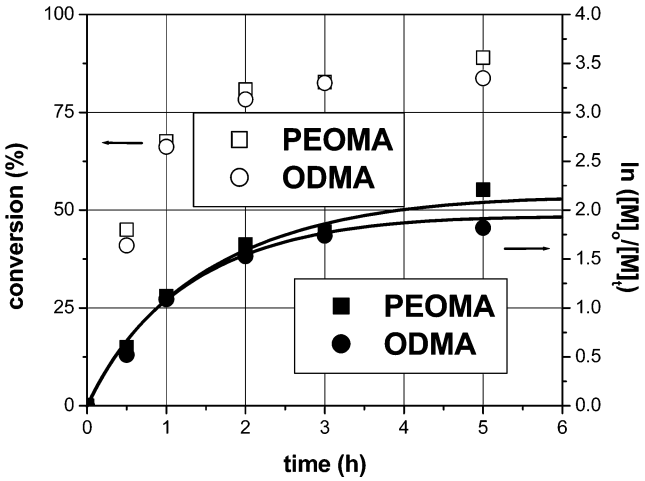

Figure 4. Plot of monomer consumption vs time for copolymerization of PEOMA with ODMA (**IV**). Conditions: [PEOMA + ODMA]$_0$:[EtBriBu]$_0$:[CuCl]$_0$:[Me$_6$TREN]$_0$ = 50 + 450:1:2:2; (PEOMA + ODMA)/(anisole + xylene) = 1/(0.25 + 0.75) w/v; T = 90 °C.

consumed at a faster rate compared to ODA and after 6 h conversion of the comonomers reached 81 and 55%, respec-

Table 3. Copolymerization of PEOMA (A) with ODA (C)

		NMR					GPC-MALLS[b]			
	PEOMA/ODA	conv (%)			DP_n		$M_n \times 10^{-3}$		DP_n	
no.[a]	wt % (mol %)	total	A	C	A	C	(g/mol)	M_w/M_n	A	C
VII	75/25 (47/53)	83.9	95.9	73.3	194	225	313.8	1.33	213	241
VIII	50/50 (23/77)	61.5	81.2	55.5	71	236	143.7	1.48	77	221
IX	25/75 (9/91)	72.2	87.6	71.1	32	328	110.7	1.63	28	310

[a] (**VII**−**IX**) $[PEOMA + ODA]_0:[EtBriBu]_0:[CuCl]_0:[Me_6TREN]_0 = 500:1:2:2$; 90 °C; mon/solv = 1/1 w/v; anisole/*o*-xylene (1/1). [b] THF, d*n*/d*c* (**VII**) = 0.07 mL/g, d*n*/d*c* (**VIII**) = 0.074 mL/g, d*n*/d*c* (**IX**) = 0.077 mL/g.

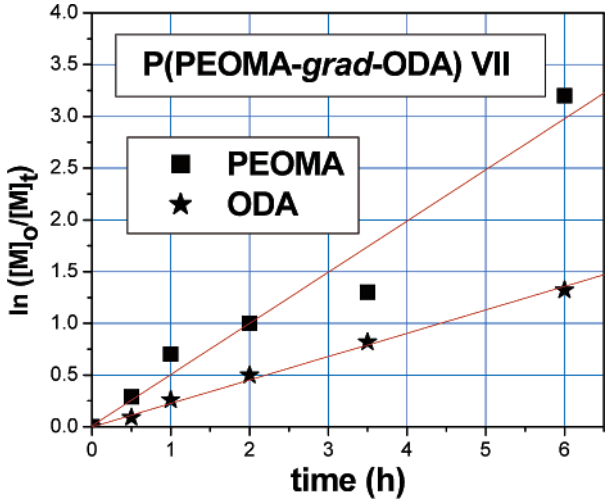

Figure 5. Plot of monomer consumption vs time for the copolymerization of PEOMA and ODA (**VII**). Conditions: $[PEOMA + ODA]_0:[EtBriBu]_0:[CuCl]_0:[Me_6TREN]_0 = 235 + 265:1:2:2$; (PEOMA + ODMA)/(anisole + *o*-xylene) = 1/(0.5 + 0.5) w/v; $T = 90$ °C.

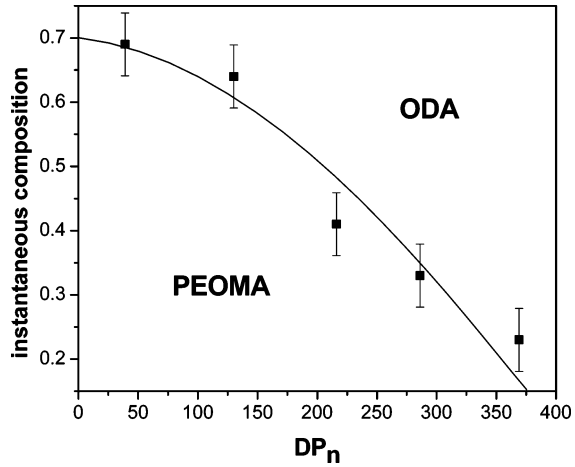

Figure 6. Instantaneous composition of P(PEOMA-*grad*-ODA) (**VII**).

tively. The PEOMA/ODA systems with various feed ratios (0.47, 0.23, and 0.09 molar fraction of PEOMA) were used for determination of the monomer reactivity ratios by the Mayo−Lewis method.[31] The higher reactivity ratio of the methacrylate than the acrylate comonomer, r_1(PEOMA) = 1.30 and r_2(ODA) = 0.58, suggested that the formed copolymer should exhibit a gradient in graft composition starting from pure PPEOMA, which gradually changes to heterosequences and finally to enriched dodecyl segments (**VII**−**IX**, Scheme 1). The plot of instantaneous composition vs chain length of copolymer calculated from conversion of the comonomers is presented in Figure 6. The errors are due to subtracting too large numbers. The average instantaneous composition decreases continuously along the chain contour from 70% PEOMA on one side of the polymer chain to 77% ODA on the other side. This confirms

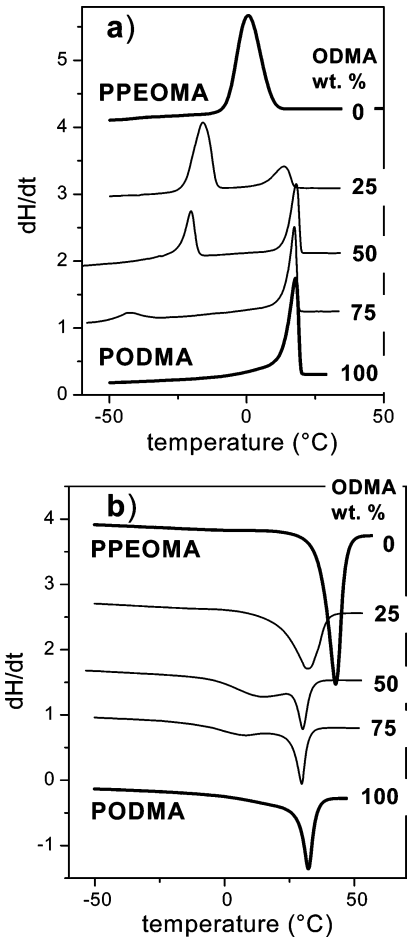

Figure 7. DSC thermograms recorded during cooling (a) and heating (b) for the random copolymers containing PEO and OD side chains. The traces for homopolymers are shown by thick lines.

the gradient structure. The overall composition of P(PEOMA-*grad*-ODA) was 49/51 (mol %). Variation in the ratio of the comonomers influenced the length of the pseudoblocks, which is shown in Table 3. Increasing amounts of ODA in the copolymer, from 25 to 75 wt % (53 to 91 mol %), significantly influenced the polydispersity index, which increased from 1.3 to 1.6. This indicates more favorable incorporation of PEOMA than ODA into the copolymer, resulting in controlled gradient copolymers with defined composition.

Behavior in Bulk. DSC Analysis. All homopolymers (PPEOMA, PODMA, PODA) and the brush copolymers (PEOMA-*ran*-ODMA and PEOMA-*grad*-ODA) started to crystallize at room temperature. The DSC traces revealed multiple crystallization and melting peaks for the copolymer samples, indicating that two crystalline phases were formed corresponding to the different constituents. Figure 7 shows the DSC results for the random copolymers (PEOMA and ODMA comonomer pair). Slightly different results for the other comonomer pair (PEOMA and ODA) are available in the Supporting Information (Figure

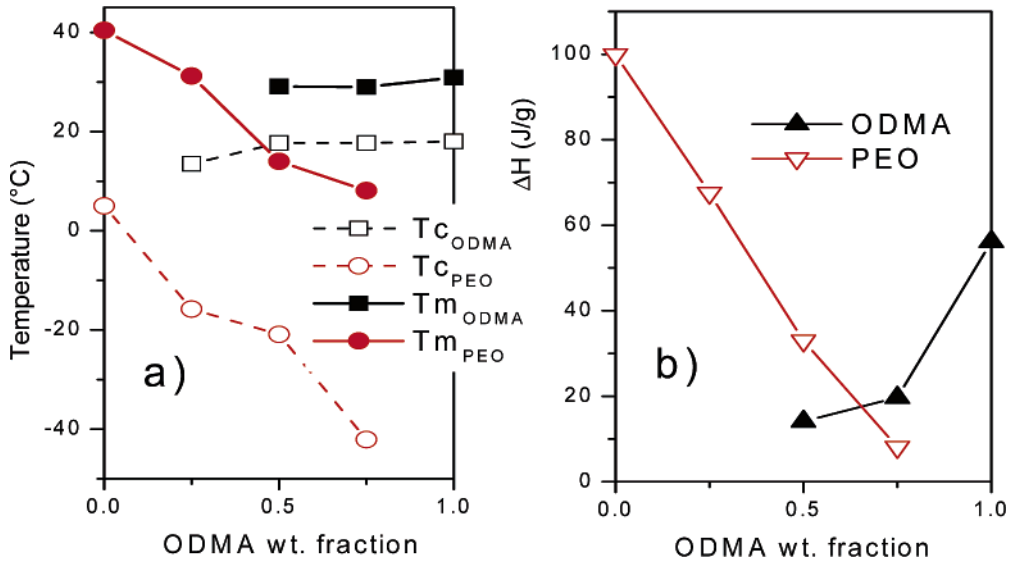

Figure 8. Composition dependencies of crystallization (T_c) and melting (T_m) temperatures (a) and melting enthalpies (b) for the homopolymers and random copolymers of PEOMA and ODMA.

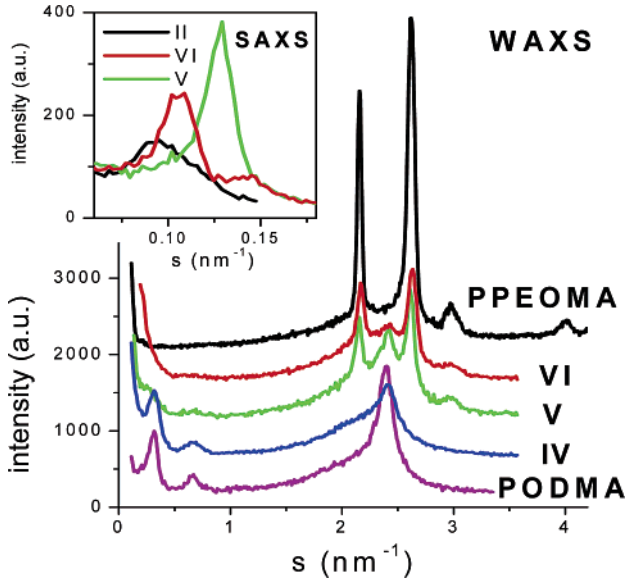

Figure 9. Wide-angle X-ray diffractograms for homopolymers random and copolymers. Inset is presented for SAXS measurements.

S1). The thermograms were obtained for cooling (crystallization) and heating (melting) runs. Under cooling, the ODMA crystallized at nearly the same temperature ($T_{c,ODMA}$ = 15−17 °C), independent of composition and with enthalpies increasing with the amount of incorporated ODMA, while the crystallization of the PEOMA segment occurred at different temperatures and with different enthalpies. Both values decreased with PEOMA content. Similar behavior was seen for melting, where the crystalline ODMA domains melt at temperature 35−37 °C. The apparent dependences of the crystallization/melting temperatures and enthalpies on the composition are illustrated in Figure 8. The corresponding results for the gradient copolymers are presented in the Supporting Information (Figure S2).

Morphology of Copolymers. The WAXS and SAXS intensity distributions recorded at room temperature for the random copolymers are shown in Figure 9, in comparison with the corresponding homopolymers PODMA (**I**) and PPEOMA (**II**). Two intense reflections were observed at 2.15 and 2.61 nm^{-1} (d = 4.6 and 3.8 Å) in the X-ray diffraction diagram in the wide-angle region and a peak of smaller intensity at 2.95 nm^{-1} (d = 3.4 Å). These reflections are related to the crystallization of PPEOMA and give information about its packing.[32] For PODMA, the presence of the first- and second-order reflections at 0.33 and 0.66 nm^{-1} (d = 30 and 15 Å) indicates a layered structure, whereas the intense peak at 2.38 nm^{-1} reveals a hexagonally packed structure of *n*-alkyl side chains with lattice spacing of 4.2 Å.[9,33] The characteristic reflections for both crystalline segments are also detected in the copolymers, where the intensity of the corresponding peaks depends on composition. Unexpectedly, the peaks corresponding to the interlayer spacing (30 Å) in PODMA structure were also present in copolymers **IV** and **V**. This could indicate that unreacted ODMA was not completely removed by ultrafiltration, and its residue coexists as a blend with the graft copolymer forming a crystallizable structure with an interlayer distance of 30 Å. The first- and second-order reflections at s = 2.15 and 2.61 nm^{-1} could be related either to crystalline PODMA side chains in the copolymer or to crystals formed from the residual ODMA.

Another interesting feature is the better resolution of the Bragg reflections from the gradient copolymers (Supporting Information, Figure S3), which means that the crystalline units are less disordered and also larger than for random sequence distribution.

The inset in Figure 9 shows the intensity distributions determined in the SAXS range for the samples **II**, **VI**, and **Vb**. The intensity maxima in SAXS diffractograms for PEOMA segments in all samples (homopolymer and random copolymers) are related to the periodicity of a superstructure. The corresponding Bragg values become smaller for smaller amounts of PEOMA segments in the copolymer. The interlayer spacing corresponds approximately to double the length of the PEO side chains ($L_{SC\ PEO,\ th}$ = 10.49 nm, simulated by Chem.3D Ultra). It suggests that the PEO helices are plausibly segregated from OD side chains and assembled on the one side of the backbone. In addition, they are not intercalated with PEO chains of the other brush macromolecules. The evolution of correlation distances d_{PEO} and d_{OD}, shown in Table 4, changes proportionally to variation in composition.

Furthermore, the X-ray diffraction, recorded at higher temperature (50−20 °C) for the random copolymer **VI** (25 wt % ODMA), demonstrates an amorphous halo, whereas at −10 °C the sample was crystalline (Figure 10a). During the heating cycle it is the opposite case, namely, the crystalline sample became amorphous at 40 °C (Figure 10b). All diffraction patterns seem

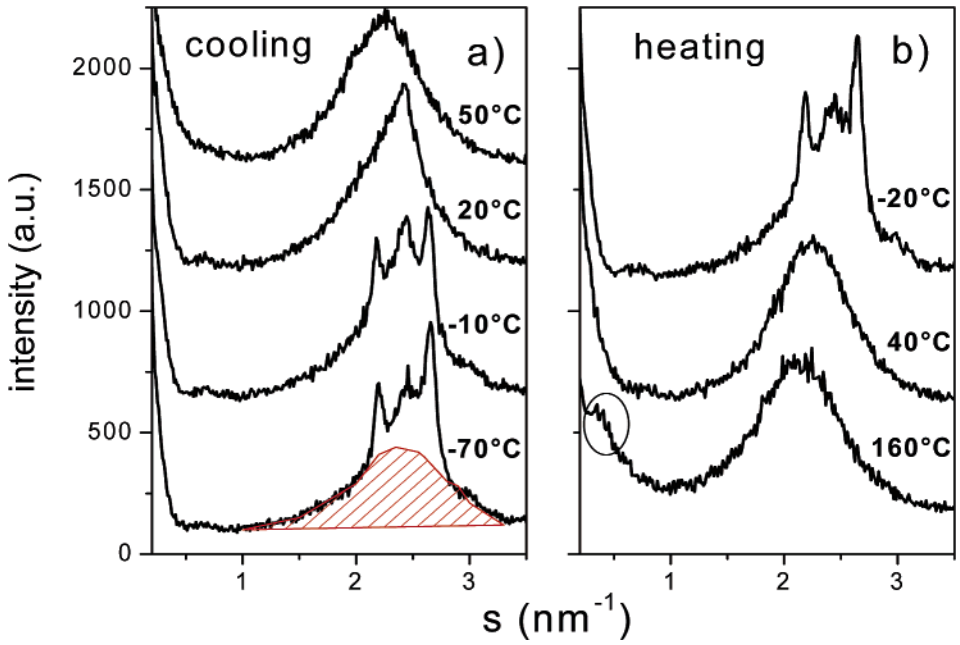

Figure 10. Wide-angle X-ray scattering during cooling (a) and heating (b) at various temperature for P(ODMA-*ran*-PEOMA) **VI** (25 wt % ODMA).

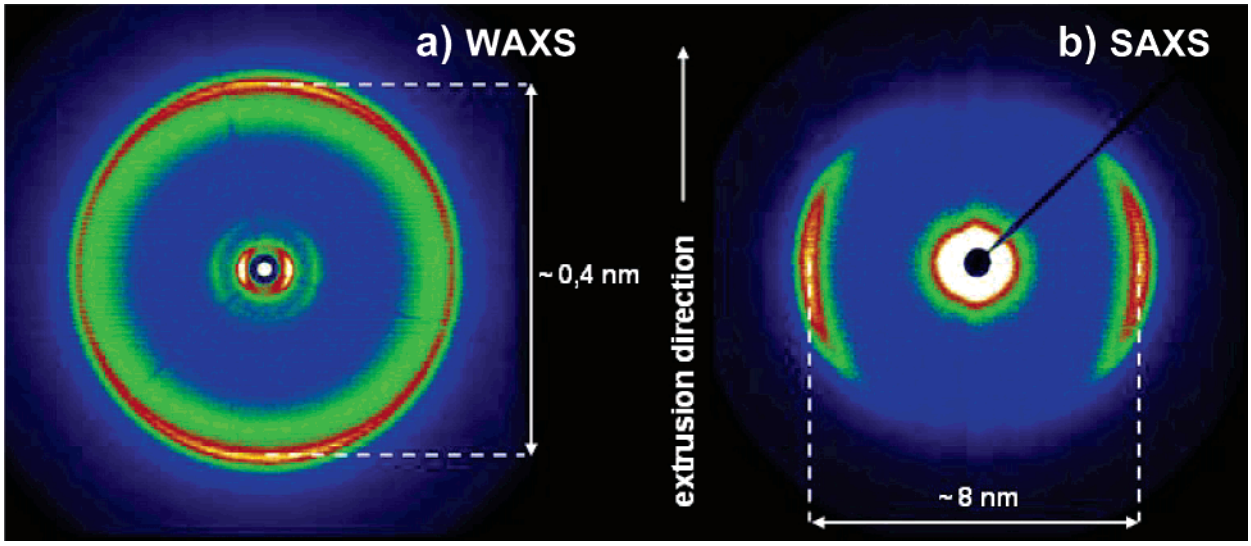

Figure 11. 2D X-ray diffraction (a) WAXS and (b) SAXS patterns for oriented samples of random copolymer **Vb** (50 wt % ODMA).

Table 4. Distances Corresponding to the SAXS Peak for Random Copolymers and Homopolymers

no.	ODMA (wt %)	s_{PEO} (nm^{-1})	d_{PEO} (nm)[a]	s_{OD} (nm^{-1})	d_{OD} (nm)[a]
Ic	100	no peak		0.329	3.04
IV	75			0.317	3.15
Vb	50	0.129	7.74	0.272	3.68
VI	25	0.109	9.19	no peak	
II	0	0.095	10.50		

[a] The quantity of d spacing is equivalent to inversed scattering vector $d = 1/s$.

to include some contribution to intensity from amorphous components. This is indicated by the hatched pattern area in Figure 10a. This made separation of the reflections corresponding to PEOMA and ODMA difficult. This assumption is confirmed by previously performed WAXS studies on the crystallization behavior of the graft copolymer, PMMA-*graft*-PEO, which indicated that the peaks corresponding to crystalline PEO side chains overlap with the amorphous halo of the PMMA backbone.[32] This observation supports a similar model for the bilayers of the graft copolymers containing PEOMA and PODMA units prepared in this work.

Additional details concerning the morphology of the structure were revealed by the 2D WAXS and SAXS patterns obtained for macroscopically oriented samples, which were obtained by extrusion. There are two kinds of reflections: the wide-angle meridional (Figure 11a) and the small-angle equatorial (Figure 11b). Extrusion of the polymers should induce orientation of the main chains along the filament axes (extrusion direction). The reflection on the meridian describes periodicities of the side chain packing equal to 0.4 nm, while the equatorial reflection is attributed to the distances between the backbones separated by the crystallized side chains. The result obtained from 2D SAXS pattern for representative sample **Vb** (~8 nm) is comparable to the value presented in Table 3.

The DSC and X-ray results suggest that crystallization in the copolymers was hindered by frustration in packing of the

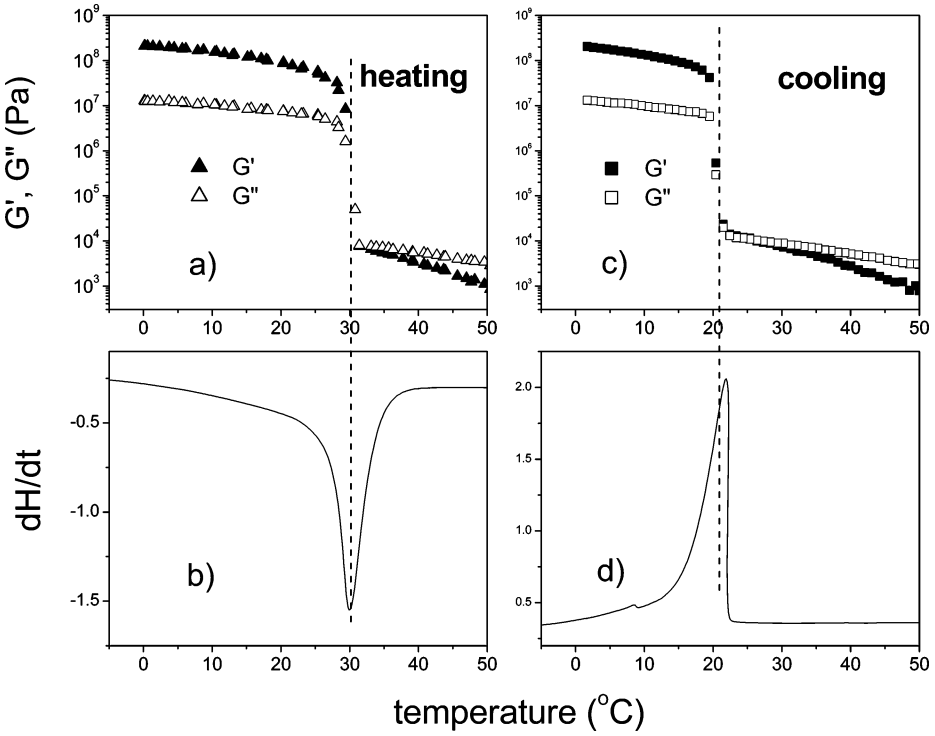

Figure 12. Mechanical characteristics (2 °C/min) and DSC traces (10 °C/min) of the PODMA **Ic** during heating (a, b) and cooling (c, d).

Scheme 2. Proposed Model for a Hypothetical Bilayer Structure Formed by Graft Copolymers P(PEOMA-*ran*-ODMA)

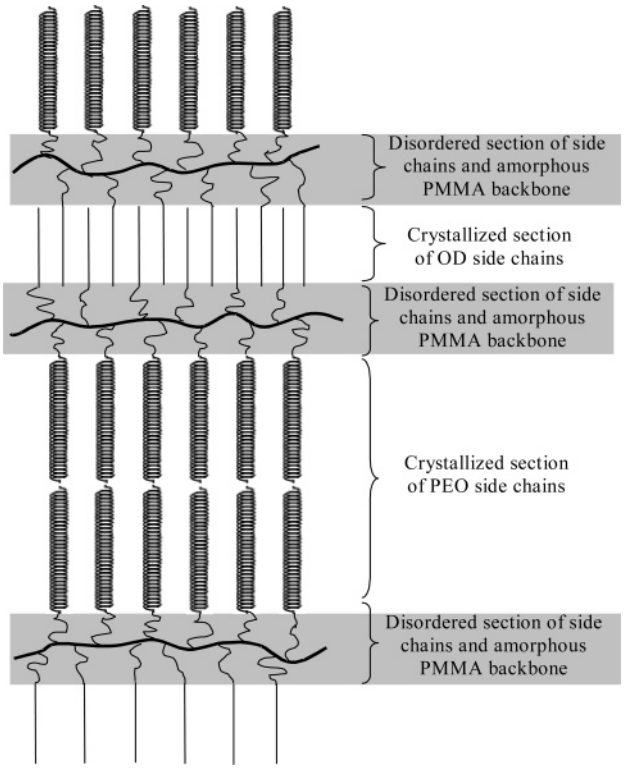

components as well as by the kinetics of the necessary phase separation processes. It was expected that the combination of two crystallizable segments, but with different chemical properties, hydrophilic PEOMA and hydrophobic ODMA, would lead to microphase segregation. The proposed model for the bilayers, which can be formed by graft copolymers P(PEOMA-*ran*-ODMA), is illustrated in Scheme 2. The scheme shows graft copolymers which have two kinds of crystallizable side chains attached to an amorphous main chain. Studies described in the literature postulate that the strongly disordered part of OD side chains includes six CH_2 units that are needed as a spacer to connect the crystalline parts of the side chains to the backbone.[33] In the case of PEO polymer, the chain has seven CH_2CH_2O units in two turns of the helix with crystallographic repeat distance of 19.2 Å and tunnel radius of 1.3−1.5 Å.[34] However, different degrees of crystallization and different modes of packing, i.e., the hexagonal packing of octadecyl side chains and the helical structure with monoclinic cell in crystalline poly(ethylene oxide), may cause frustration in the packing of the semicrystalline copolymer. The consequence can be formation of amorphous layers instead of semicrystalline ODMA segments in the graft copolymers. However, this could not be definitively proven because of the presence of residual monomer that formed crystals as well as units which are embedded in the polymer.

The morphology was also analyzed by polarized optical microscopy (POM), which demonstrated a fine spherulitic structure of PPEOMA[35] when the sample was crystallized from the isotropic melt isothermally. In the case of all copolymers, and PODMA itself, it was not possible to observe any morphology which can be explained by presence of large amounts of much smaller spherulites below the size of optical resolution. The POM images are presented in the Supporting Information as Figure S4.

Dynamic mechanical experiments were performed in the molten states of the samples to characterize their viscoelastic behavior. Temperature dependencies of the real (G') and imaginary (G'') parts of the shear modulus were determined over a broad temperature range. The main hardening/softening transition in the PODMA sample (**Ic**), related to the melting (Figure 12a) or the crystallization (Figure 12c), was comparable with transition temperatures determined by DSC (Figure 12b,d). Shear modulii, G' and G'', show typical values for crystalline polymeric materials, i.e., about 10^8 and 10^7 Pa, respectively. The difference of the transition temperatures between DSC and mechanical-dynamical tests was caused by the different cooling/heating rates, which were applied to the sample.

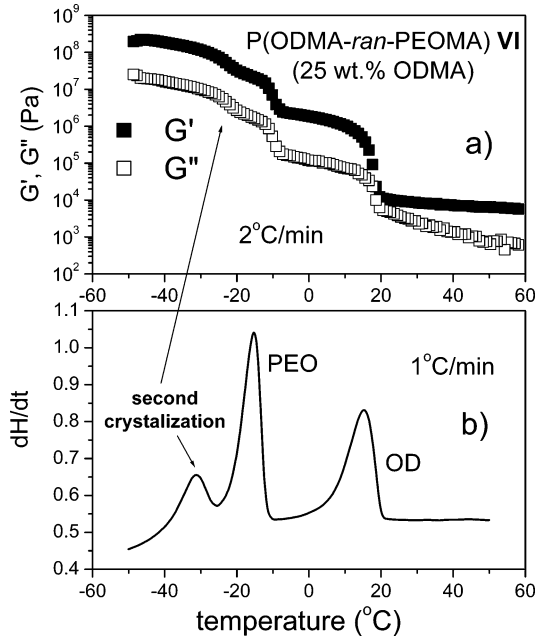

Figure 13. Mechanical characteristics (a) and DSC thermogram (b) for P(ODMA-*ran*-PEOMA) containing 25 wt % ODMA (**VI**) during cooling.

The mechanical behavior during cooling of the representative random copolymer with 25 wt % (50 mol %) ODMA (**VI**) is shown in Figure 13a. Transitions corresponding to crystallization of OD side chains at 20 °C and PEO segments at −10 °C were observed. The reason for a third small jump of the shear modulus at −25 °C is not clearly defined, and it was not present in the initial DSC results, where only two peaks were observed (Figure 7a). Because the rate of temperatures change may strongly influence the formation of the crystalline phases in the copolymers, an additional DSC was conducted at a heating rate of 1 °C/min for the same copolymer (**VI**). The result is illustrated in Figure 13b, which shows one extra peak at low temperature (−30 °C) besides two peaks assigned to the crystallization of PEO ($T_{c,PEO} = -13$ °C) and OD ($T_{c,OD} = 17$ °C) phases. It is supposed that phase separation continued to occur slowly at low temperature, and it could initiate a secondary crystallization process.

The copolymer systems, similar to PEOMA homopolymer, show elastic properties at high temperature ($G' > G''$) even above the melting point and remain in the range characteristic for supersoft elastomers ($10^3 < G' < 10^4$ Pa). It indicates that these materials are not thermally stable and can cross-link at high temperature. In fact, when samples containing mole fractions of PEOMA are heated above ∼80 °C (depending on the composition), they become insoluble. Cross-linking was also observed after a longer time of storage at room temperature.

Conclusion

The crystallizable monomers, PEOMA and ODMA or ODA, were copolymerized via *grafting through* by ATRP, yielding densely heterografted amphiphilic polymers containing ethyleneoxy ($DP_{sc} = 23$) and aliphatic octadecyl side chains with various compositions. Random copolymers were prepared using two methacrylates (PEOMA/ODMA). Gradient copolymers were formed from methacrylate/acrylate (PEOMA/ODA) comonomers. Various initial ratios of comonomers yielded polymers with more or less distributed PEO grafts. Copolymerization conducted in the presence of a CuBr/dNbpy catalyst system led to relatively low monomer conversion (∼60%) and to polymers with $DP_n \sim 300$. However, when CuCl/Me_6TREN was used as the catalyst complex, the DP_n of the copolymers reached ∼400−480 repeating units (above 80% monomer conversion) with polydispersity indices $M_w/M_n = 1.1-1.4$ for random and $M_w/M_n = 1.3-1.6$ for gradient copolymers. Additionally, homopolymers PODMA ($DP_n = 165-435$, $M_w/M_n = 1.15-1.3$), PODA ($DP_n = 145$, $M_w/M_n = 1.5$), and PPEOMA ($DP_n \sim 400$, $M_w/M_n < 1.1$) were synthesized and compared with the copolymers.

Both of the graft copolymer segments PEO and OD undergo crystallization at room temperature. The ability to form well-oriented structures allows one to retrieve values for backbone−backbone distance and between side chains by X-ray methods. The composition of the copolymer strongly influences the morphology. Spherulitic crystallization was observed for the homopolymer sample of PPEOMA. Furthermore, PEOMA homopolymer and its copolymers with ODMA show elastic properties at high temperature ($G' > G''$), which renders them potential candidates for soft rubbers ($10^3 < G' < 10^4$ Pa).

Acknowledgment. The authors thank Prof. S. Sheiko (University of North Carolina at Chapel Hill) for GPC-MALLS data. D.N. acknowledges the Max Planck Society for a scholarship and is grateful to Dr. Y. Zhang for helpful discussions.

Supporting Information Available: Thermal properties and X-ray analysis of the gradient copolymers; images of polarized optical microscopy for PPEOMA. This material is available free of charge via the Internet at http://pubs.acs.org.

References and Notes

(1) Plate, N. A.; Shibaev, V. P.; Petrukhin, B. S.; Zubov, Y. S.; Kargin, V. A. *J. Polym. Sci.* **1971**, *A9*, 2291.
(2) Plate, N. A.; Shibaev, V. P. *J. Polym. Sci., Makromol. Rev.* **1974**, *8*, 117.
(3) Hsieh, H. W. S.; Post, B.; Morawetz, H. *J. Polym. Sci.* **1976**, *14*, 1241.
(4) Magagnini, P. L.; Andruzzi, F.; Benetti, G. F. *Macromolecules* **1980**, *13*, 12.
(5) Andruzzi, F.; Lupinacci, D.; Magagnini, P. L. *Macromolecules* **1980**, *13*, 15.
(6) Segre, A. L.; Andruzzi, F.; Lupinacci, D.; Magagnini, P. L. *Macromolecules* **1981**, *14*, 1845.
(7) Baskar, G.; Ramya, S.; Mandal, A. B. *Colloid Polym. Sci.* **2002**, *280*, 886.
(8) Yokota, K.; Hirabayashi, T.; Inai, Y. *Polym. J.* **1994**, *26*, 105.
(9) Inomata, K.; Sakamaki, Y.; Nose, T.; Sasaki, S. *Polym. J.* **1996**, *28*, 986.
(10) Beers, K. L.; Matyjaszewski, K. *J. Macromol. Sci., Pure Appl. Chem.* **2001**, *38*, 731.
(11) Qin, S.; Matyjaszewski, K.; Xu, H.; Sheiko, S. S. *Macromolecules* **2003**, *36*, 605.
(12) Qin, S.; Saget, J.; Puyn, J.; Jia, S.; Kowalewski, T.; Matyjaszewski, K. *Macromolecules* **2003**, *36*, 8969.
(13) Jakubowski, W.; Lutz, J.-F.; Slomkowski, S.; Matyjaszewski, K. *J. Polym. Sci., Part A: Polym. Chem.* **2005**, *43*, 1498.
(14) Street, G.; Illsley, D.; Holder, S. J. *J. Polym. Sci., Part A: Polym. Chem.* **2005**, *43*, 1129.
(15) Wang, J. S.; Matyjaszewski, K. *J. Am. Chem. Soc.* **1995**, *117*, 5614.
(16) Matyjaszewski, K.; Xia, J. *Chem. Rev.* **2001**, *101*, 2921.
(17) Kamigaito, M.; Ando, T.; Sawamoto, M. *Chem. Rev.* **2001**, *101*, 3689.
(18) Klumperman, B.; Chambard, G.; Brinkhuis, R. H. G. *Advances in Controlled/Living Radical Polymerization; ACS Symp. Ser.* **2003**, *854*, 180.
(19) Neugebauer, D.; Zhang, Y.; Pakula, T.; Matyjaszewski, K. *Polymer* **2003**, *44*, 6863.
(20) Neugebauer, D.; Matyjaszewski, K. *Congr. Proc. MACRO 2004* (*IUPAC Conf.*) **2004**, 2.1.6, 1251.
(21) Neugebauer, D.; Zhang, Y.; Pakula, T.; Sheiko, S. S.; Matyjaszewski, K. *Macromolecules* **2003**, *36*, 6746.
(22) Koji, I.; Junichiro, S.; Atsushi, S. *J. Colloid Interface Sci.* **2004**, *274*, 472.
(23) Deimede, V.; Kallitsis, J. K. *Chem.—Eur. J.* **2002**, *8*, 467.
(24) Neugebauer, D.; Zhang, Y.; Pakula, T.; Matyjaszewski, K. *Macromolecules* **2005**, *38*, 8687.

(25) Pakula, T.; Matyjaszewski, K. *Nat. Mater.*, submitted for publication.
(26) Floudas, G.; Tsitsilianis, C. *Macromolecules* **1997**, *30*, 4381.
(27) Floudas, G.; Reiter, G.; Lambert, O.; Dumas, P. *Macromolecules* **1998**, *31*, 7279.
(28) Matyjaszewski, K.; Patten, T. E.; Xia, J. *J. Am. Chem. Soc.* **1997**, *119*, 674.
(29) Queffelec, J.; Gaynor, S. G.; Matyjaszewski, K. *Macromolecules* **2000**, *33*, 8629.
(30) Gromada, J.; Spanswick, J.; Matyjaszewski, K. *Macromol. Chem. Phys.* **2004**, *205*, 551.
(31) Mayo, F. R.; Lewis, F. M. *J. Am. Chem. Soc.* **1944**, *66*, 1594.
(32) Yao, N. *J. Macromol. Sci., Phys.* **1991**, *B30*, 225.
(33) Arndt, T.; Schouten, A. J.; Schmidt, G. F.; Wegner, G. *Makromol. Chem.* **1991**, *192*, 2215.
(34) Takahashi, Y.; Tadokoro, H. *Macromolecules* **1973**, *6*, 672.
(35) Yang, H.; Yin, W.; Zhang, X.; Cai, Z.; Wang, Z.; Cheng, R. *J. Appl. Polym. Sci.* **2005**, *96*, 2454.

MA051702H